J Radioanal Nucl Chem (2016) 309:947–953
DOI 10.1007/s10967-016-4744-2

# Feasibility study of FLUKA Monte Carlo simulation for a beta-emitting brachytherapy source: dosimetric parameters of $^{142}$Pr glass seed

**Marzieh Anjomrouz[1] · Mo K. Bakht[2] · Mahdi Sadeghi[3]**

Received: 19 May 2015 / Published online: 4 March 2016


**Abstract** A series of dosimetric calculations and modeling should be done before the clinical use of any new brachytherapy source. In this work, the capability of the FLUKA Monte Carlo code to simulate praseodymium-142 glass seed as a beta-emitting brachytherapy source was evaluated. The reference dose rate, target dose rate, radial dose function and the anisotropy function were estimated. The agreement between the reported radiochromic film measurements and the FLUKA code outputs indicated that FLUKA as a multipurpose Monte Carlo simulation code can be used to predict the required dosimetric parameters reasonably well.

**Keywords** Brachytherapy · Dosimetry · FLUKA · Monte Carlo · Praseodymium-142

## Introduction

Beta-particle emitter praseodymium-142 [$T_{1/2} = 19.12$ h] is gaining importance as an emerging therapeutic agent in nuclear medicine and interstitial brachytherapy [1, 2]. The radionuclide $^{142}$Pr decays via $\beta^-$ emission with a maximum energy of 2.162 MeV to the ground state of $^{142}$Nd (with a probability of 96.3 %). There is also a second $\beta^-$ emission with a maximum energy of 0.586 MeV and a subsequent gamma emission with an energy of 1.576 MeV (with probability 3.7 %). These particles penetrate approximately 3 mm of soft tissue; therefore, high-energy $\beta^-$ emissions of $^{142}$Pr can be used for high penetration in large tumors. Previously, a promising *$^{142}$Pr glass seed* for prostate cancer brachytherapy with a simple structure was proposed [3, 4]. $^{142}$Pr glass seed has several advantages over the conventional seeds. For instance, the absorbed dose in adjacent organs could be minimized as a result of the short range of beta particles. Moreover, because of high density and high atomic number of Pr-glass, a radio-opaque marker was not necessary [4]. Also, a $^{142}$Pr capillary tube-based radioactive implant (CTRI) has been suggested as a $^{142}$Pr source with approximately similar dosimetric parameters to $^{142}$Pr glass seed [5].

Furthermore, the American Association of Physicists in Medicine (AAPM) has recommended that before using each new brachytherapy source clinically, dosimetric characteristics of all such sources must be determined by two independent methods: theoretical calculations and experimental measurements. The aim of using these methods is providing reliable data for treatment planning calculations and dose prescriptions. As AAPM Task Group 43 (TG-43) and its updated version (TG-43U1) used for gamma emitter sources, AAPM Task Group 60 (TG-60) along with the updated version (Report-149) has recommended a dosimetry protocol that includes dose calculation formalism for beta-emitting brachytherapy sources [6–10].

A variety of general-purpose Monte Carlo codes are currently available to calculate dose distribution with high spatial resolution around brachytherapy sources. These

✉ Mahdi Sadeghi
msadeghi@nrcam.org

1 Department of Radiology, University of Otago, Christchurch, New Zealand

2 Laboratory of Molecular Imaging and Therapy, Cancer Research Institute, Seoul National University College of Medicine, Seoul, Korea

3 Radiation Application Research School, Nuclear Science and Technology Research Institute, P.O. Box: 14395-836, Tehran, Iran

codes utilize modern cross-section libraries and a sufficiently complete model of photon scattering, absorption, and secondary photon creation while the main difference between them originates from some criteria of electron and positron transport simulations such as boundary-crossing and step-size artifacts as applied by different scattering algorithms. However, very close agreement between their results has been reported by investigators only if the source emission spectrum, the seed geometry, and the assigned materials are implemented extremely similarly [6]. In general, the dosimetric calculations by modeling sources in the water phantom using Monte Carlo N-Particle Transport (MCNP) Code [11] as a well-established Monte Carlo simulation code have been performed to fulfill the requirements according to AAPM recommendations [12–20]. It is noteworthy that the other Monte Carlo radiation transport simulation codes such as EGSnrc, EGS4, GEANT4, GATE, PENELOPE, ETRAN, CYLTRAN codes could also be benchmarked against the experimental measurements for medical physics and nuclear medicine proposes [6, 21, 22].

The general-purpose Monte Carlo code FLUKA is maintained and developed by collaboration of the Italian Institute for Nuclear Physics (INFN) and the European Organization for Nuclear Research (CERN). This code is aimed for the calculation of particle transport and interactions with matter [23, 24]. Up to now, in the field of medical physics, FLUKA has mostly been dedicated to radiation protection [25–28], beam collimation [29, 30], and hadrontherapy [31–33]. Additionally, this code has facilitated optimization of target design and the activation study of the medical radioisotopes [34–36].

Furthermore, it has been shown that FLUKA Monte Carlo code provides reliable results when transporting electrons in the low energy range [37], being proved as a suitable code for nuclear medicine dosimetry [38]. The purpose of this study is to determine how well the Monte Carlo particle transport code FLUKA can simulate $^{142}$Pr glass seed as a sample beta-emitting brachytherapy source. Moreover, this code enables us to score the energy deposited around the source in comparison with the reported experimental measurements and the MCNP5 Monte Carlo code simulation data.

## Theory

### $^{142}$Pr glass seed description

The Pr glass seed has a simple homogeneous cylinder structure. This seed was manufactured by MO-SCI Corporation (Rolla, MO 65402), in which praseodymium oxide was added to the glass materials ($Al_2O_3$ and $SiO_2$). The density of Pr glass was 4.0 g/cm$^3$ and the weight percent of Pr was 44.5 %. Pr glass seed was a solid cylinder with a diameter of 0.8 mm as shown in Fig. 1, the same as the typical seeds such as $^{125}$I. However, the length was twice that of the typical seeds to achieve the target dose at the edges of the field and to shorten surgery time [3, 4].

### Monte Carlo simulation

In this work, the $^{142}$Pr sources surrounded by the soft tissues has been simulated by considering a $^{142}$Pr sources in a water phantom such as prostate tumors. Thereby, the simulation results could be satisfactory due to the similarity of the involved parameters such as specific Bremsstrahlung constant in water and the soft tissues [39]. In addition, MCNP5 simulation was used for $^{142}$Pr-glass seed by Jung et al. [3] to benchmark MCNP5 calculations against the experimental measurement. In the Jung et al. [3] study, the ITS energy-indexing algorithm was used to transport beta particles. This algorithm provided dose distribution closer to the actual data by assigning the data from the average energy group [4].

In this work, to simulate $^{142}$Pr glass seed placed in center of a water phantom and to extract dosimetry parameters, version 2011.2.14 (updated in 11$^{th}$ December 2012) of the FLUKA code has been used [23]. The FLUKA database contains all $^{142}$Pr decays as already has explained in introduction section. Mostly for isotopes decay simulation in FLUKA code, a threshold is applied and decays with branching ratio smaller than 0.1 % are discarded. In addition, the emission probabilities are conserved on average. In order to transport charged particles, FLUKA utilizes a multiple scattering algorithm based on Moliere's theory amended by Bethe [40]. The Moliere multiple scattering model is applicable for electrons with minimum

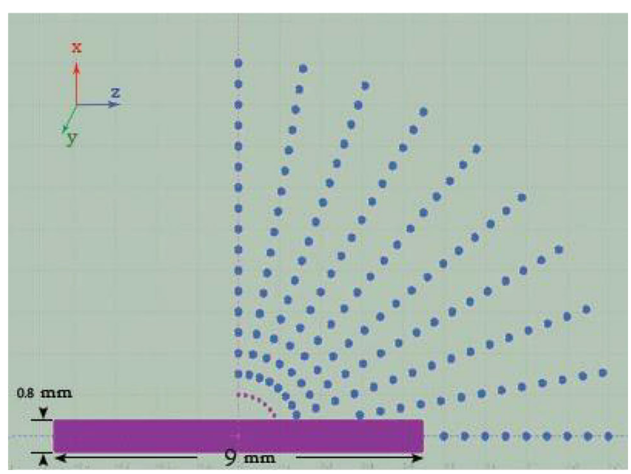


**Fig. 1** $^{142}$Pr glass seed dimensions in a schematic view of the simulated scoring geometry with the coordinate system

energy of 20–30 keV in high-Z materials. Whereas single-scattering algorithm is an alternative approach which can be used to transport electron in segmental and complex geometry accurately, where the electron has to pass through various boundaries. In addition, it would provide the acceptable results in any material particularly in low energy range. The single-scattering algorithm is available by setting MULSOPT card, explicitly [41]. To simulate energy and angular distribution of bremsstrahlung photons in this work, the differential cross section of Seltzer and Berger was used [23, 38, 42].

## FLUKA setting

A useful option has been embedded in BEAM card called ISOTOPE. By combination use of this option and HI-PROPE card to determine the type of isotope, the code uses relevant spectrum to input file from own databases, conveniently. FLUKA isotope database generated by National Nuclear Data Center at Brookhaven National Library enables us to simulate the emission spectrum of beta emission isotopes [24, 38]. In this work, by choosing the radio-lanthanide $^{142}$Pr in HI-PROBE, beta spectrum of this isotope was loaded for FLUKA input file.

Also, some other cards such as RADDECAY are required to simulate the radioactive decays of prompt and decay particles.

Regarding with energy threshold for all electron and photon interactions, EM-CASCA option was chosen to take into account the electromagnetic cascades interactions along with disabling neutron interactions options which are unnecessary in this work [20].

In addition, the types of interaction as well as the adequate thresholds were set in the physics and transport sections of this code. To set the energy thresholds for electron and photon production in different materials, and electron and photon transport cutoffs in selected regions, EMFCUT was chosen and adjusted, explicitly. If the transport cutoffs in a considered region are greater than those of production in a given material, particles with energies higher than production thresholds and lower than transport cutoffs are not transported, however they are still produced [23]. Hence, in this work, production and transport thresholds were set to the same value of 10 keV kinetic energy plus 511 keV for the rest mass of electron and positron (overall 521 keV). Also, the photons energy cut-off was assigned 1 keV. Besides, the energy thresholds for Compton and photoelectric were considered 10 keV. In fact, the energy cut-offs are adjusted for fulfilment of the interactions influencing electron dose. Thus, the interactions which do not have any significant impacts on the electron doses such as coherent scattering are not considered since their transportation could increase CPU time without any merit.

In FLUKA, size of election steps is set corresponding to a fixed fraction of total energy [38]. By choosing a default option, implicitly the maximum fraction of total energy to be lost in a step can be adjusted 20 %. However, according to FLUKA instructions, achieving high level of accuracy (5–10 %) in some problems such as dosimetry and in thin-slab geometries is recommended [23]. Adjusting this parameter is also applicable by activating EMFFIX option, explicitly. Therefore, in this simulation we selected EMFFIX card to override step length of 7 % in the water, in which enough accuracy obtained as well as not being too CPU-time consuming.

Furthermore, the card of DCYSCORE was embedded in the scoring setup and then linked to the dose estimator of USRBIN. This code was set at $4 \times 10^8$ of initial photon histories in order to minimize statistical uncertainties of simulation varied from $6 \times 10^{-4}$ % up to 1 % with increasing distance from source.

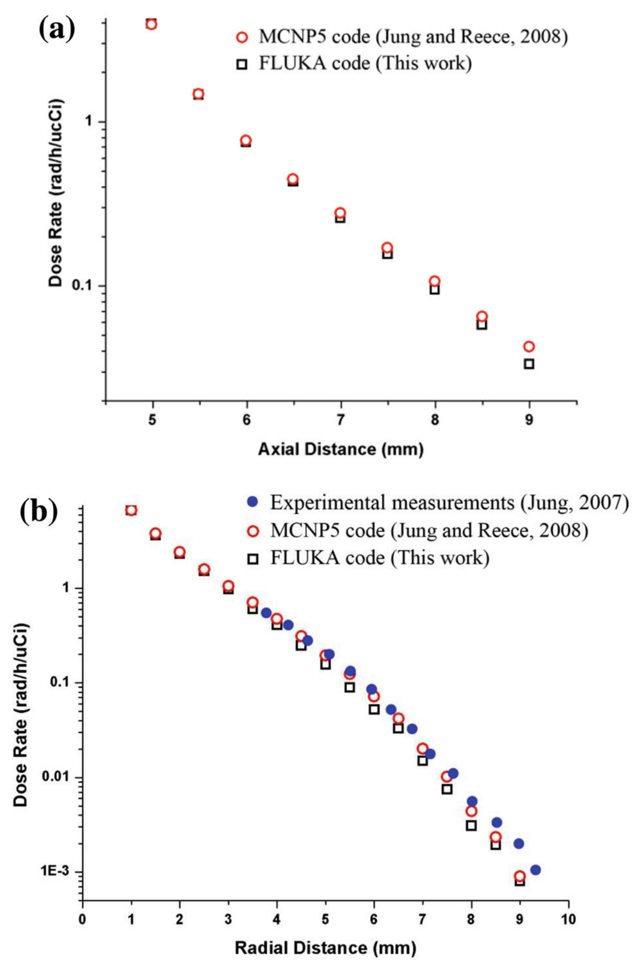


**Fig. 2** The calculated axial and radial dose profiles of $^{142}$Pr glass seed

**Table 1** The look-up dose rate for $^{142}Pr$ glass seed

| | θ(°) | | | | | | | | | |
|---|---|---|---|---|---|---|---|---|---|---|
| r(mm) | 90 | 80 | 70 | 60 | 50 | 40 | 30 | 20 | 10 | 0 |
| 1 | 6.72E+00 | 6.84E+00 | 7.08E+00 | 7.42E+00 | 9.20E+00 | 1.14E+01 | 1.57E+01 | | | |
| 1.5 | 3.65E+00 | 3.88E+00 | 4.04E+00 | 4.77E+00 | 5.35E+00 | 7.09E+00 | 9.61E+00 | 1.59E+01 | | |
| 2 | 2.32E+00 | 2.49E+00 | 2.65E+00 | 3.03E+00 | 3.53E+00 | 4.72E+00 | 6.69E+00 | 1.09E+01 | | |
| 2.5 | 1.53E+00 | 1.58E+00 | 1.72E+00 | 1.99E+00 | 2.44E+00 | 3.20E+00 | 4.80E+00 | 8.15E+00 | | |
| 3 | 9.86E−01 | 1.00E+00 | 1.12E+00 | 1.38E+00 | 1.71E+00 | 2.39E+00 | 3.55E+00 | 6.43E+00 | 1.57E+01 | |
| 3.5 | 6.04E−01 | 6.85E−01 | 7.47E−01 | 9.40E−01 | 1.15E+00 | 1.63E+00 | 2.61E+00 | 4.70E+00 | 1.20E+01 | |
| 4 | 4.10E−01 | 4.18E−01 | 4.83E−01 | 5.88E−01 | 8.21E−01 | 1.17E+00 | 1.85E+00 | 3.39E+00 | 9.30E+00 | |
| 4.5 | 2.50E−01 | 2.67E−01 | 3.10E−01 | 4.20E−01 | 5.24E−01 | 8.35E−01 | 1.25E+00 | 2.10E+00 | 4.96E+00 | |
| 5 | 1.57E−01 | 1.60E−01 | 1.99E−01 | 2.45E−01 | 3.50E−01 | 5.35E−01 | 8.20E−01 | 1.32E+00 | 2.28E+00 | 3.88E+00 |
| 5.5 | 8.95E−02 | 1.02E−01 | 1.28E−01 | 1.56E−01 | 2.24E−01 | 3.66E−01 | 5.36E−01 | 7.99E−01 | 1.17E+00 | 1.44E+00 |
| 6 | 5.25E−02 | 5.47E−02 | 7.27E−02 | 9.65E−02 | 1.48E−01 | 2.26E−01 | 3.39E−01 | 5.11E−01 | 6.58E−01 | 7.40E−01 |
| 6.5 | 3.31E−02 | 4.33E−02 | 4.09E−02 | 5.91E−02 | 9.64E−02 | 1.37E−01 | 2.03E−01 | 3.24E−01 | 3.79E−01 | 4.28E−01 |
| 7 | 1.50E−02 | 1.56E−02 | 2.40E−02 | 3.19E−02 | 5.67E−02 | 9.54E−02 | 1.37E−01 | 1.88E−01 | 2.40E−01 | 2.56E−01 |
| 7.5 | 7.48E−03 | 8.11E−03 | 1.22E−02 | 1.91E−02 | 3.04E−02 | 5.49E−02 | 8.67E−02 | 1.17E−01 | 1.43E−01 | 1.55E−01 |
| 8 | 3.09E−03 | 3.58E−03 | 6.32E−03 | 9.54E−03 | 1.82E−02 | 3.29E−02 | 5.05E−02 | 7.18E−02 | 9.05E−02 | 9.43E−02 |
| 8.5 | 1.95E−03 | 1.56E−03 | 2.89E−03 | 4.94E−03 | 9.96E−03 | 1.89E−02 | 2.99E−02 | 4.16E−02 | 5.34E−02 | 5.79E−02 |
| 9 | 8.03E−04 | 8.60E−04 | 1.19E−03 | 2.21E−03 | 4.76E−03 | 1.00E−02 | 1.72E−02 | 2.57E−02 | 3.21E−02 | 3.33E−02 |

**Table 2** Comparison of the dose rate at reference and target point obtained by different calculation methods

| Dose point | Dose rate (cGy/h/μCi) | | |
|---|---|---|---|
| | Experimental measurements [3] | MCNP5code [3] | FLUKA code (This work) |
| $r = 2$ mm, $\theta = 90°$ | NA[a] | 2.412 ± 0.01 | 2.324 ± 0.017 |
| $r = 6$ mm, $\theta = 90°$ | 0.045 | 0.072 ± 0.002 | 0.053 ± 0.043 |

[a] Not applicable (the dose rate is beyond the sensitivity of the radiochromic film)

Figure 1 shows the simulated geometry by FLUKA, illustrating the seed and detectors in water on $y$–$z$ plane. Similar to the previous study [3, 4], a cylindrical $^{142}Pr$ source was modeled in a spherical water phantom. Each detector array encompassing water spheres with a radius of 0.1 mm was placed in the same distance but various angels from 0° to 90° in steps of 10° and whole arrays were positioned from 1 mm to 9 mm by 0.5 mm increments.

Finally, to obtain the required doses, the USRBIN cards were set for all of the detectors. It is noteworthy that the input file was run using a personal computer with dual-core CPU and Linux™ operating system. Additionally, the radiation dose in the assigned detectors was accessible with average error of well under $5.4 \times 10^{-2}$ %.

## Results

Figure 2 illustrates the calculated axial and radial dose profiles of $^{142}Pr$ glass seed by FLUKA in comparison with the reported MCNP5 data.

### Reference dose rate

Table 1 shows the look-up dose rate. The reference point recommended in AAPM TG-60 is $r_0 = 2$ mm and $\theta_0 = 90^0$. The dose rate at reference point $D(r_0, \theta_0)$ and a target point ($r_0 = 6$ mm and $\theta_0 = 90^0$) derived based on two-dimensional dose distributions in water are presented in Table 2. According to this table, FLUKA result at ($r_0 = 6$ mm and $\theta_0 = 90^0$) 17 % differs from the measurement whereas the discrepancy between measurement and MCNP5 is 60 %. Thus, at target point, the estimated data by the FLUKA code are closer to the experimental measurements as compared with MCNP5 data. However, the uncertainties of MCNP5 are less than FLUKA.

### Radial dose function, $g_L(r)$

Radial dose function, $g_L(r)$ describes the effect of tissue attenuation on dose distribution in the transverse plane of a brachytherapy source that is centered at the coordinate origin [6]. The values of $^{142}Pr$ glass seed radial dose function $g_L(r)$ were calculated using the FLUKA code and are presented on Fig. 3.

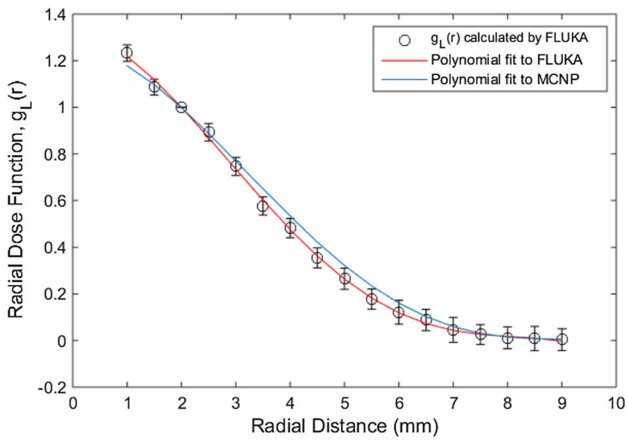


**Fig. 3** The radial doses function of $^{142}Pr$ glass seed

In addition, a fifth order polynomial fit on the FLUKA radial dose function in water for a range of $r$ values from 1 to 9 mm follows the Eq. (1).

$$g_L(r) = a_0 + a_1 r + a_2 r^2 + a_3 r^3 + a_4 r^4 + a_5 r^5 \quad (1)$$

Table 3 presents the fifth-order polynomial coefficients obtained by a regression fit to FLUKA data as compared to MCNP5 coefficients. Moreover, to evaluate the goodness of fit, we calculated the coefficient of determination and mean square error (MSE) [43, 44] which are 0.99922 and 0.000175, respectively.

## Anisotropy function, $F(r, \theta)$

Dose variations due to the distribution of radioactivity within the source, self-absorption and oblique filtration of the radiation in the encapsulating material are described by the 2D anisotropy function [6]. In this study, anisotropy function was calculated to three decimal places as presented in Table 4. The maximum value of the this function

**Table 3** The estimated 5th order polynomial coefficients by two simulated codes

| Coefficient | MCNP5 [3] | FLUKA (this work) | SE of fitting to FLUKA[a] |
|---|---|---|---|
| $a_0$ | 1.2623376 | 1.3249500 | 0.0185 |
| $a_1$ | −0.0187000 | −0.0253000 | 0.2775 |
| $a_2$ | −0.0735998 | −0.0939900 | 0.1560 |
| $a_3$ | 0.0087016 | 0.0134200 | 0.0392 |
| $a_4$ | −0.0000594 | −0.0003211 | 0.0044 |

[a] *SE* standard error

**Table 4** FLUKA calculated Anisotropy function, $F(r, \theta)$ of $^{142}Pr$ glass seed with the uncertainty of ±0.005

| | $\theta$(°) | | | | | | | | | |
|---|---|---|---|---|---|---|---|---|---|---|
| $r$(mm) | 90 | 80 | 70 | 60 | 50 | 40 | 30 | 20 | 10 | 0 |
| 1 | 1.000 | 1.000 | 0.982 | 0.943 | 1.019 | 1.030 | 1.085 | | | |
| 1.5 | 1.000 | 1.044 | 1.028 | 1.108 | 1.077 | 1.153 | 1.182 | 0.697 | | |
| 2 | 1.000 | 1.053 | 1.058 | 1.101 | 1.106 | 1.186 | 1.259 | 0.840 | | |
| 2.5 | 1.000 | 1.010 | 1.040 | 1.096 | 1.160 | 1.216 | 1.354 | 0.960 | | |
| 3 | 1.000 | 0.999 | 1.056 | 1.191 | 1.274 | 1.418 | 1.561 | 1.143 | 1.936 | |
| 3.5 | 1.000 | 1.114 | 1.152 | 1.329 | 1.416 | 1.607 | 1.924 | 1.334 | 2.413 | |
| 4 | 1.000 | 1.003 | 1.102 | 1.237 | 1.512 | 1.753 | 2.114 | 1.690 | 2.985 | |
| 4.5 | 1.000 | 1.054 | 1.166 | 1.468 | 1.622 | 2.136 | 2.502 | 1.736 | 3.367 | |
| 5 | 1.000 | 1.007 | 1.197 | 1.380 | 1.763 | 2.271 | 2.811 | 2.078 | 3.565 | 3.830 |
| 5.5 | 1.000 | 1.124 | 1.356 | 1.551 | 2.015 | 2.831 | 3.459 | 2.294 | 4.361 | 4.457 |
| 6 | 1.000 | 1.029 | 1.319 | 1.655 | 2.312 | 3.095 | 3.986 | 2.894 | 5.185 | 5.290 |
| 6.5 | 1.000 | 1.295 | 1.184 | 1.625 | 2.446 | 3.077 | 4.004 | 3.451 | 5.545 | 5.898 |
| 7 | 1.000 | 0.468 | 0.697 | 0.884 | 1.463 | 2.210 | 2.857 | 3.442 | 8.695 | 8.914 |
| 7.5 | 1.000 | 1.073 | 1.570 | 2.361 | 3.518 | 5.773 | 8.314 | 5.026 | 11.378 | 11.926 |
| 8 | 1.000 | 1.147 | 1.976 | 2.874 | 5.165 | 8.566 | 12.145 | 6.539 | 18.664 | 18.994 |
| 8.5 | 1.000 | 0.794 | 1.434 | 2.374 | 4.538 | 7.970 | 11.769 | 9.598 | 18.461 | 19.644 |
| 9 | 1.000 | 1.064 | 1.445 | 2.304 | 4.674 | 9.222 | 15.153 | 9.757 | 28.212 | 28.879 |

is 28.879 obtained at farthest distance ($\theta = 0°$, $r = 9$ mm) and the estimated value using MCNP5 was 32.863 at the same position as it can be found in Ref [3]. This high value range for anisotropy function at maximum distance is due to the length of Pr glass seed which is twice of commercial seeds such as I-125 as mentioned before.

## Discussion

Dose rate calculation around the seed indicates that the FLUKA and the MCNP5 data are in agreement particularly in angles from 0° to 40° at distances up to 0.5 cm. In this area, discrepancies are at most 8 % as compared to higher angles which have maximum of 35 % difference. In larger distances and the higher radial angles, more uncertainties influence dose rate as a result of dropping beta emissions intensity. Similarly, MCNP5 dose rate could also be influenced by this issue. The electron transport simulations may suffer from some issues such as boundary crossing artifacts and electron step size [6]. Also, using dedicated library and given threshold setting in each Monte Carlo code could result in forming various structures for particle transport. However, to optimize results and minimize discrepancies, proportional setting and effective thresholds has been adjusted in current work.

In general, agreement between FLUKA outputs and other valid data clarifies that FLUKA code can be applied to perform dosimetry data set as a supplementary tool similar to MCNP5. It should be said that increasing the number of regions cause to boost the running time required to handle particle transportation. Therefore, the interactions which do not have any considerable effect on the electron doses should be eliminated to prevent increasing process time.

Finally, it should be mentioned that $^{142}$Pr glass seed is not a pure beta-emitting brachytherapy source. However, the gamma energy contribution to dose as a fraction of total dose is insignificant [3, 4]. Therefore, in this manuscript gamma dosimetric parameters including the air-kerma strength, the absorbed dose rate constant and the air-kerma rate since are not reported.

## Conclusions

In this work, the general-purpose Monte Carlo particle transport code FLUKA was used to simulate $^{142}$Pr glass seed as a beta-emitting brachytherapy source. Agreement between the reported experimental measurements and the FLUKA code results was satisfying and showed that FLUKA can predict the recommended AAPM dosimetric parameters appropriately. Moreover, the accessibility and user-friendly graphical interface as practical features can make this code privileged.

**Acknowledgments** The authors would like to express their best appreciation to Dr. Jae Won Jung of Department of Physics, East Carolina University, Greenville, North Carolina, USA for providing the necessary experimental data and his valuable suggestions. In addition, the authors would like to thank Mr. Alberto Fassò from Jefferson Lab, Newport News, VA, USA, Dr. Paola Sala of Istituto Nazionale di Fisica Nucleare (INFN), Milano, Italy and Dr. Pooneh Saidi for their helpful comments in this study.

## References

1. Bakht MK, Sadeghi M (2011) Internal radiotherapy techniques using radiolanthanide praseodymium-142: a review of production routes, brachytherapy, unsealed source therapy. Ann Nucl Med 25(8):529–535
2. Bakht MK, Sadeghi M, Ahmadi SJ, Sadjadi SS, Tenreiro C (2013) Preparation of radioactive praseodymium oxide as a multifunctional agent in nuclear medicine: expanding the horizons of cancer therapy using nanosized neodymium oxide. Nucl Med Comm 34(1):5–12. doi:10.1097/MNM.1090b1013e32835aa32837bd
3. Jung JW, Reece WD (2008) Dosimetric characterization of $^{142}$Pr glass seeds for brachytherapy. Appl Radiat Isot 66(4):441–449. doi:10.1016/j.apradiso.2007.11.008
4. Jung JW (2007) $^{142}$Pr glass seeds for the brachytherapy of prostate cancer. Ph D, Texas A&M University, Texas
5. Bakht MK, Sadeghi M, Ahmadi SJ, Haddadi A, Sadjadi S, Tenreiro C (2013) Monte Carlo simulations and radiation dosimetry measurements of $^{142}$Pr capillary tube-based radioactive implant (CTRI): a new structure for brachytherapy sources. Ann Nucl Med. doi:10.1007/s12149-013-0683-y
6. Chiu-Tsao ST, Schaart DR, Soares CG, Nath R (2007) Dose calculation formalisms and consensus dosimetry parameters for intravascular brachytherapy dosimetry: recommendations of the AAPM Therapy Physics Committee Task Group No. 149. Med Phys 34(11):4126–4157
7. Nath R, Amols H, Coffey C, Duggan D, Jani S, Li Z, Schell M, Soares C, Whiting J, Cole PE, Crocker I, Schwartz R (1999) Intravascular brachytherapy physics: report of the AAPM Radiation Therapy Committee Task Group no. 60. American Association of Physicists in Medicine. Med Phys 26(2):119–152
8. Rivard MJ, Coursey BM, DeWerd LA, Hanson WF, Huq MS, Ibbott GS, Mitch MG, Nath R, Williamson JF (2004) Update of AAPM Task Group No. 43 Report: a revised AAPM protocol for brachytherapy dose calculations. Med Phys 31(3):633–674
9. Nath R, Anderson LL, Luxton G, Weaver KA, Williamson JF, Meigooni AS (1995) Dosimetry of interstitial brachytherapy sources: recommendations of the AAPM Radiation Therapy Committee Task Group No. 43. American Association of Physicists in Medicine. Med Phys 22(2):209–234
10. Venselaar J, Meigooni AS, Baltas D, Hoskin PJ (Eds) (2012) Comprehensive brachytherapy: physical and clinical aspects. Taylor & Francis, Abingdon
11. Briesmeister JF (2000) MCNPTM–A General Monte Carlo N-Particle Transport Code. Version 4C, LA-13709-M, Los Alamos National Laboratory
12. Selvam TP, Nagarajan PS, Rajan KN, Sethulakshmi P, Bhatt BC (2003) A semi-analytic approach to determine dose rate constant of brachytherapy sources in compliance with AAPM TG 60 formalism. Australas Phys Eng Sci Med 26(4):179–184

13. Bernard S, Vynckier S (2005) Dosimetric study of a new polymer encapsulated palladium-103 seed. Phys Med Biol 50(7):1493–1504
14. Dauffy LS, Braby LA, Berner BM (2005) Dosimetry of the 198Au source used in interstitial brachytherapy. Med Phys 32(6): 1579–1588
15. Sadeghi M, Hosseini SH, Raisali G (2008) Experimental measurements and Monte Carlo calculations of dosimetric parameters of the IRA1-103Pd brachytherapy source. Appl Radiat Isot 66(10): 1431–1437
16. Parsai EI, Zhang Z, Feldmeier JJ (2009) A quantitative three-dimensional dose attenuation analysis around Fletcher-Suit-Delclos due to stainless steel tube for high-dose-rate brachytherapy by Monte Carlo calculations. Brachytherapy 8(3):318–323
17. Sadeghi M, Taghdiri F, Hosseini SH, Tenreiro C (2010) Monte Carlo calculated TG-60 dosimetry parameters for the beta-emitter 153Sm brachytherapy source. Med Phys 37(10):5370–5375
18. Gialousis G, Dimitriadis A, Yakoumakis E (2011) Monte Carlo estimation of dose difference in lung from 192Ir brachytherapy due to tissue inhomogeneity. Radiat Prot Dosimetry 147(1–2):287–290
19. Saidi P, Sadeghi M, Shirazi A, Tenreiro C (2010) Monte Carlo calculation of dosimetry parameters for the IR08-$^{103}$Pd brachytherapy source. Med Phys 37:2509–2515
20. Asadi S, Masoudi SF, Shahriari M (2012) The effects of variations in the density and composition of eye materials on ophthalmic brachytherapy dosimetry. Med Dosim 37(1):1–4
21. Uusijarvi H, Chouin N, Bernhardt P, Ferrer L, Bardies M, Forssell-Aronsson E (2009) Comparison of electron dose-point kernels in water generated by the Monte Carlo codes, PENELOPE, GEANT4, MCNPX, and ETRAN. Cancer Biother Radiopharm 24(4):461–467
22. Papadimitroulas P, Loudos G, Nikiforidis GC, Kagadis GC (2012) A dose point kernel database using GATE Monte Carlo simulation toolkit for nuclear medicine applications: comparison with other Monte Carlo codes. Med Phys 39(8):5238–5247
23. Battistoni G, Cerutti F, Fasso A, Ferrari A, Muraro S, Ranft J, Roesler S, Sala P (2007) The FLUKA code: description and benchmarking. In: AIP Conference Proceedings, p 31
24. Fasso A, Ferrari A, Ranft J, Sala P (2005) FLUKA: A multi-particle transport code CERN-2005-10 (2005). INFN/TC-05/11, SLAC
25. Patni HK, Akar DK, Nadar MY, Ghare VP, Rao DD, Sarkar PK (2013) Estimation of specific absorbed fractions for selected organs due to photons emitted by activity deposited in the human respiratory tract using ICRP/ICRU male voxel phantom in fluka. Radiat Prot Dosimetry 153(1):32–46
26. Nemati MJ, Habibi M, Amrollahi R (2012) Analysis of concrete labyrinth shielding and radiation dose for APF plasma focus neutron source by FLUKA Monte Carlo code. J Radioanal Nucl Chem 1:221–226
27. Nemati MJ, Amrollahi R, Habibi M (2012) Analysis for radiation and shielding dose in plasma focus neutron source using FLUKA. J Fusion Energy 31(3):284–297
28. Demir N, Tarim U, Popovici M-A, Demirci Z, Gurler O, Akkurt I (2013) Investigation of mass attenuation coefficients of water, concrete and bakelite at different energies using the FLUKA Monte Carlo code. J Radioanal Nucl Chem 298(2):1303–1307. doi:10.1007/s10967-013-2494-y
29. Kimstrand P, Tilly N, Ahnesjö A, Traneus E (2008) Experimental test of Monte Carlo proton transport at grazing incidence in GEANT4, FLUKA and MCNPX. Phys Med Biol 53(4):1115–1129
30. Battistoni G, Cappucci F, Bertolino N, Brambilla MG, Mainardi HS, Torresin A (2012) FLUKA Monte Carlo simulation for the Leksell Gamma Knife Perfexion radiosurgery system: homogeneous media. Physica Med 29:656–661
31. Song HS, Kim HW, Zhou T, Lee BN, Lee YS, Lee SH, Choi HJ, Yeon YH, Oh JH, Gad KM, Kadi Y, Chai JS (2011) Computer simulation of CNT field emitter based X-ray spectra using with FLUKA code. J Korean Phys Soc 59(23):1999–2001
32. Battistoni G, Broggi F, Brugger M, Campanella M, Carboni M, Cerutti F, Colleoni P, D'Ambrosio C, Empl A, Fassò A, Ferrari A, Ferrari AN, Gadioli E, Lantz M, Lee K, Lukasik G, Mairani A, Margiotta A, Mauri M, Morone MC, Mostacci A, Muraro S, Parodi K, Patera V, Pelliccioni M, Pinsky L, Ranft J, Roesler S, Rollet S, Sala PR, Sarchiapone L, Sioli M, Smirnov G, Sommerer F, Theis C, Trovati S, Villari R, Vinke H, Vlachoudis V, Wilson T, Zapp N (2008) The FLUKA code and its use in hadron therapy. Nuovo Cimento Soc Ital Fis, C 31(1):69–75
33. Rinaldi I, Collaboration OBOTF (2014) SU-E-T-323: the FLUKA Monte Carlo code in ion beam therapy. Med Phys 41(6):298
34. Mokhtari Oranj L, Kakavand T, Sadeghi M, Aboudzadeh Rovias M (2012) Monte Carlo FLUKA code simulation for study of 68 Ga production by direct proton-induced reaction. Nucl Instru Methods Phys Res Sect A 677:22–24
35. Infantino A, Cicoria G, Pancaldi D, Ciarmatori A, Boschi S, Fanti S, Marengo M, Mostacci D (2011) Prediction of $^{89}$Zr production using the Monte Carlo code FLUKA. Appl Radiat Isot 69(8):1134–1137
36. Remetti R, Burgio NT, Maciocco L, Arcese M, Filannino MA (2011) Monte Carlo simulation and radiometric characterization of proton irradiated [$^{18}$O]H2O for the treatment of the waste streams originated from [$^{18}$F]FDG synthesis process. Appl Radiat Isot 69(7):1046–1051
37. Fasso A, Ferrari A, Sala P (2001) Electron-photon transport in FLUKA: status. In: King et al (eds) Advanced Monte Carlo for radiation physics, particle transport simulation and applications, p 159. Springer, Lisbon
38. Botta F, Mairani A, Battistoni G, Cremonesi M, Di Dia A, Fassò A, Ferrari A, Ferrari M, Paganelli G, Pedroli G, Valente M (2011) Calculation of electron and isotopes dose point kernels with fluka Monte Carlo code for dosimetry in nuclear medicine therapy. Med Phys 38(7):3944–3954
39. Bakht MK, Jabal-Ameli H, Ahmadi SJ, Sadeghi M, Sadjadi S, Tenreiro C (2012) Bremsstrahlung parameters of praseodymium-142 in different human tissues: a dosimetric perspective for 142 Pr radionuclide therapy. Ann Nucl Med 26(5):412–418
40. Bethe H (1953) Moliere's theory of multiple scattering. Phys Rev 89(6):1256
41. Ferrari A, Sala P, Guaraldi R, Padoani F (1992) An improved multiple scattering model for charged particle transport. Nucl Instrum Methods Phys Res, Sect B 71(4):412–426
42. Seltzer SM, Berger MJ (1985) Bremsstrahlung spectra from electron interactions with screened atomic nuclei and orbital electrons. Nucl Instrum Methods Phys Res, Sect B 12(1):95–134
43. Lang TA, Secic M (2006) How to report statistics in medicine: annotated guidelines for authors, editors, and reviewers. ACP Press, New York. ISBN 1930513690
44. Ahsanullah M (2003) Focus on applied statistics. Nova Publishers, New York. ISBN 1590339118